Rev.Adv.Mater.Sci. 17(2008) 62-70

CORRELATION BETWEEN THERMAL TREATMENT AND TETRAGONAL/MONOCLINIC NANOSTRUCTURED ZIRCONIA POWDER OBTAINED BY SOL–GEL PROCESS

V. Santos[1], M. Zeni[1], C.P. Bergmann[2] and J.M. Hohemberger[3]

[1] Department of Chemistry and Physics, University of Caxias do Sul, C. P. 1352, 95020-972, Caxias do Sul, RS, Brazil

[2] Department of Materials, Engineering School, Federal University of Rio Grande do Sul, Laboratory of Ceramic Materials (LACER), Osvaldo Aranha, 99, 90035-190, Porto Alegre, Brazil

[3] Federal University of Pampa, Carlos Barbosa s/n, 96412-420, Bagé, RS, Brazil

Received: January 13, 2008

Abstract. The purpose of this paper was to investigate the correlation between thermal treatment and tetragonal/monoclinic nanostructured zirconia powders obtained by sol–gel process. The originality of this work is in the evaluation of the temperature influence on the preparation of nanostructured zirconia powders. The structure of the zirconia produced is amorphous when the samples are heated below 400 °C. The zirconia powders were prepared using zirconium *n*-propoxide diluted in *n*-propanol under stirring and refluxed under controlled temperature at *p*H=5. The resulting gel was air-dried and annealed under air atmosphere at temperatures up to 800 °C for 12 h. The zirconia powders were characterized by means of differential thermal analysis, thermogravimetric analysis, X-ray diffraction, size distribution by laser diffraction, Fourier transform infrared spectroscopy, and scanning and transmission electron microscopy. Crystallite size was calculated by single-line technique using the mathematical function Pearson VII. The presence of the tetragonal phase was observed at a temperature higher than 400 °C. The monoclinic phase was formed at 600 °C, which resulted in a lowering of the content of tetragonal phase. At 800 °C, the particle showed D_{50}=11.54 μm. The crystallite size was calculated using X-ray diffraction-single line and measured by TEM, both approximately 30 nm.

1. INTRODUCTION

The development of nanotechnology both as an independent and highly interdisciplinary research field has brought great expectations in Material Science because a wide variety of materials with novel physical and chemical properties can be obtained, as well as important technological improvements can be achieved with the use of nanostructured materials. Over the past several years, a number of techniques have been developed for the production of ceramic nanoparticles. They are produced by elaborated methods that use normally sophisticated techniques, such as chemical vapor deposition [1], laser ablation [2], aerosol [3], hypersonic plasma [4], plasma spray [5], and spray pyrolysis [6]. However, the synthesis of these ceramics using wet-chemical routes such as co-precipitation [7], combustion synthesis [8] and sol–gel [9], has also been reported. The last technique has been used in this study.

Considering the development of new materials, the experimental conditions can be adjusted in order to get stable or metastable compounds. The use of high temperature to obtain crystals, glasses, or ceramics is necessary for such a process to be successful. At low temperatures, it is possible to obtain crystalline composites through polyanion preparation from solutions or even through trough hydrothermal processes. In both situations, the thermodynamic laws, which can be represented by

Corresponding author: V. Santos, e-mail: vsantos2@ucs.br

phase diagrams [10], govern the properties of the solid materials. Contrary to the conventional synthesis methods, which generally require high temperatures, the sol–gel process [11,12] makes possible the development of nanocrystals at room temperature. The great success of the sol–gel process is related to the characteristics of the materials that can be produced, such as highly porous materials [13]. These materials have potential applications in a number of processes, such as gas separation, micro- and ultrafiltration, and support of catalytic converter in the petrochemical industry, among others [14].

There has been an increase in the use of aluminium, zirconium, or titanium alkoxide in order to obtain novel materials. Most studies performed in this field focused on the synthesis of materials with mixed composition [15-19]. The physical and chemical properties of mixed oxides prepared through sol–gel process have been of great interest due to their high thermal and chemical stability. Besides, they are highly acidic because of the presence of the OH groups on the surface [17].

The formation and transformation of crystalline phases and thereby the catalytic properties of zirconia depend on synthetic parameters such as type of precursor, *p*H during hydrolysis, doping with ions, and the technique used for its synthesis followed by post-thermal treatments. The influence of various synthetic parameters on the structural and textural properties of zirconia gel has been studied [20-23].

There have been several reports on different routes of synthesis of zirconium oxide. Due to its high hardness and corrosion resistance, several studies have been carried out in order to test different synthesis possibilities [24,25]. The most appropriate experimental condition seems to be the one that hydrolyzes tetra-*n*-propoxide zirconium, including the preparation of thin oxide films, which allows for the control of the structure, morphology, and mechanical properties of the oxide. Bokhimi *et al.* [26] have prepared zirconia powder using sol–gel process with zirconium *n*-butoxide under different hydrolysis conditions (HCl, H_2SO4, CH_3COOH, and NH_4OH). Nanostructured powders were obtained after annealing and tetragonal and monoclinic zirconia nanophases were crystallized from amorphous structure. The tetragonal and/or monoclinic phases were formed at the initial crystallization stage, as a function of solution *p*H. It could be controlled during the hydrolysis by using acids as catalysts.

Several attempts have been made to obtain the metastable tetragonal and cubic phases by doping zirconia with a variety of metal oxides such as CaO, MgO, Y_2O_3, CeO_2, Ce_2O_3, La_2O_3, CuO, MnO_2, NiO, Cr_2O_3, and SnO_2. Researchers have explained the formation of these metastable phases at low temperature by various theories involving stabilization due to the defects/atomic vacancies in the lattice created by the presence of this lower valent doped metal ions [27-35].

The purpose of this study is to investigate the correlation between thermal treatment and tetragonal/monoclinic nanostructured zirconia powders obtained by sol–gel process using zirconium *n*-propoxide as precursor.

2. EXPERIMENTAL

Preparation of Zirconia powder

Zirconia powder was obtained through continuous stirring and reflux of 1 mol *n*-propanol (Merck), $1.21 \cdot 10^{-2}$ mol zirconium *n*-propoxide (Du Pont), $8.8 \cdot 10^{-2}$ mol acetic acid (Merck), and 0.71 mol deionized water for 28 h at 70 °C. The resulting *p*H was 5. The gels were then kept at room temperature (25 °C) for 48 h. The gels dried were annealed in air oven at different temperatures, ranging from 200 °C to 800 °C, for 12 h.

Characterization of Zirconia powder

X-ray diffraction (XDR) was performed on synthesized and annealed powders for phase identification and examination at a rate of 1 °C min^{-1} and crystallite size determination by peak scanned (104) at rate of 0.02 °C min^{-1} were performed, using Cu Kα radiation with a Philips X-ray diffractometer (model X'Pert MPD). Chromia was also employed as an external standard for correction due to instrumental broadening. The width of XRD peaks observed is a convolution of the factors such as inaccuracy of the instruments and physical factors such as crystallite sizes and defects [36]. The use of peak-broadening analysis for this concept is well known and it has its optimal sensitivity for materials with a mean crystal size smaller than about 0.1 μm, which is the area of interest concerning nanotechnology [36]. Crystallite sizes were obtained by X-ray diffraction line broadening through single-line plot, assuming Pearson VII profile for size contribution. These data were analyzed using the Win Fit software (version 1.2.1).

Thermogravimetric (TGA) and thermodifferential (DTA) analysis of the zirconia powder were car-

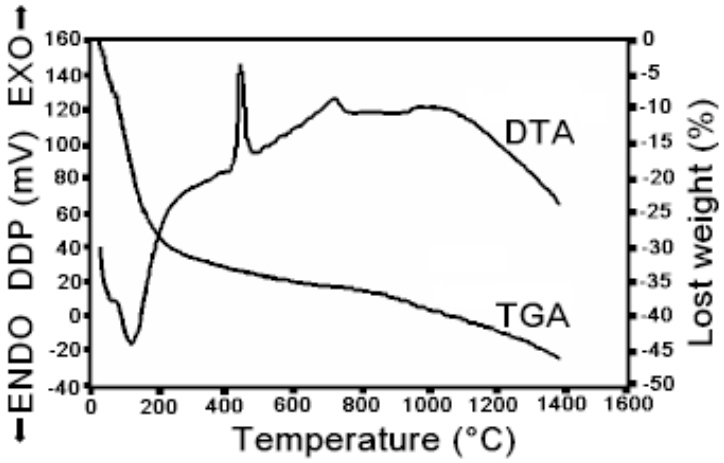

Fig. 1. Thermal analysis of zirconia powder obtained by sol-gel process.

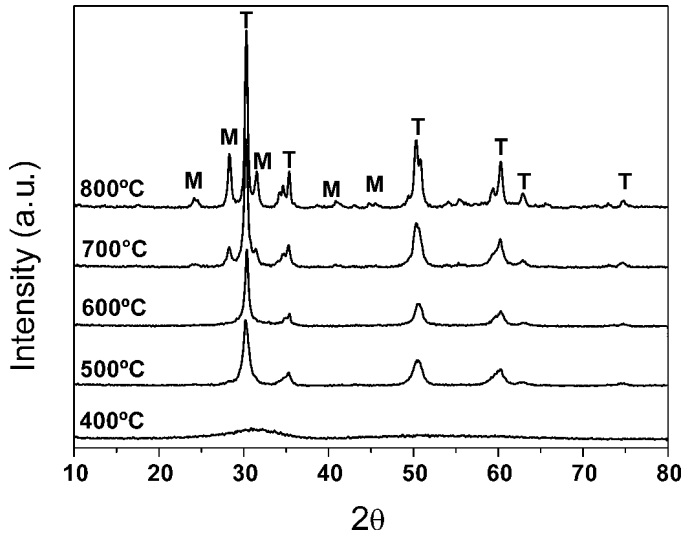

Fig. 2. Diffraction patterns of ZrO_2 calcined between 400 °C and 800 °C for 12 h at the maximum temperature, (T) tetragonal and (M) monoclinic phase.

ried out with a heating rate of 10 K min^{-1} until 1000 °C, with a flux of O_2 and N_2 at the rate of 15 mL min^{-1} and 50 mL min^{-1}, respectively. The surface of the samples were covered with gold in a diode-sputtering Baltec SCD050 coater and were observed in a Jeol JSM 5800 scanning electron microscope (SEM) at an accelerating voltage of 20 kV. Transmission electron microscopy (TEM) micrographs were recorded from a Jeol (model JEM-2010) instrument. Samples for TEM were dispersed in isopropyl alcohol through an ultrasonic bath, and a drop of suspension of each powder was deposited on carbon-coated grids.

Fourier transform infrared spectroscopy (FT-IR) analysis of dried and annealed powders were carried out in an Impact 400, Nicolet spectrometer in the wavenumber range 400–4000 cm^{-1} at resolution of 4 cm^{-1} for studying the chemical groups. For this analysis, KBr pellets were pressed to hold the samples to be analyzed.

3. RESULTS AND DISCUSSION

Fig. 1 shows the thermogravimetric and the thermodifferencial analysis of the zirconia powder obtained using sol–gel technique; a considerable weight loss can be observed in the range from 40 °C to 200 °C, probably due to dehydration. It is followed by an endothermic peak (energy used to release volatile compounds). An exothermic peak

Table 1. Phases identification of ZrO_2 annealed at different temperatures.

Temperature (°C)	Phases
400	Tetragonal
500	Tetragonal
600	Tetragonal and Monoclinic
700	Tetragonal and Monoclinic
800	Tetragonal and Monoclinic

followed by a weight loss at approximately 450 °C is observed. This is a typical behavior for combustion of organic compounds. After 450 °C, another exothermic peak is observed, but not followed by any weight loss. It could be attributed to the allotropic transformation of zirconia from tetragonal to monoclinic, which is confirmed by X-ray diffraction. The samples were submitted to a heat treatment procedure with heating rate of 5 °C min^{-1} for 12 h. Thermal analyses (DTA-TG) of the zirconium alcoholic solutions prepared by sol–gel process by stirring of zirconium *n*-propoxide (ZNP) with propanol (P3) and propanol and nitric acid (P4) in anhydrous nitrogen atmosphere show that the powders P3 and P4 have a very different behavior with respect to the thermal treatment [37]. For P3, two overlapping exothermic peaks at 300 and 350 °C may be observed, corresponding to the elimination of chemically bound water and burning of organic groups, respectively. The next peak at 480 °C is associated with the nucleation of the amorphous material to form the pure ZrO_2 tetragonal polymorph. At higher temperatures, a broad exothermic peak corresponding to the metastable tetragonal (t) to monoclinic transformation (m) is observed. The endothermic peak at approximately 1100 °C indicates the equilibrium transition m $\rightarrow$ t. For P4, two marked exothermic peaks at 350 and 450 °C that would correspond to the elimination of organic groups and monoclinic phase crystallization, respectively, are observed. This phase appears at lower temperatures compared with P3. The TG of P4 does not indicate any weight loss for temperatures higher than 450 °C and the DTA does not show the endothermic peak of the equilibrium transition m $\rightarrow$ t [37].

The data obtained from X-ray diffraction of the annealed powder as function of treatment temperature are shown in Table 1. Fig. 2 shows the X-ray diffraction patterns after annealing at the temperatures of 400 °C and 800 °C for the synthesis conditions investigated in this study; it was possible to observe the presence of the tetragonal phase (T), 27-0997 Zirconium Oxide, above 400 °C. This phase is metastable below 1170 °C [26]. When acetic acid was used as the hydrolysis catalyst, the tetragonal zirconia nanophase was more stable, according to Bokhimi. A model was proposed for explaining the stabilization of the tetragonal phase. In this model, OH^- ions and Zr vacancies in the crystalline structure were the stabilizers. The model also explained the irreversible structure transformation of the tetragonal to monoclinic phase, which was observed when samples were annealed [26]. The tetragonal phase is stable even at 400 °C because of the reduction of the surface energy, which is caused by low-sized crystallites. In a previous study [38], it was observed by X-ray diffraction that zirconia had an amorphous structure, before annealing at 400 °C. It transforms to tetragonal structure before annealing [26,38]. After further heat treatment at 500 °C, the zirconia maintains the tetragonal phase structure. At 600 °C, the formation of the monoclinic phase (M), 07-0343 Baddeleyite, takes place, lowering the content of tetragonal phase. This is probably due to the increase of the crystallite size as function of temperature in agreement with the *Garvie* Theory [17]. Thus, from 600 to 800 °C, zirconia exists in both tetragonal and monoclinic phases.

Caruso *et al.* [37] observed that P3 powder exhibited monoclinic phase as the unique phase, with main peaks at $2\theta = 28.21°$ and $2\theta = 31.51°$, and P4 retained a fraction of tetragonal phase, $2\theta \approx 30°$, after heat treatment of both powders at 1000 °C for 1 h.

Bhagwat *et al.* [39] observed the powder XRD patterns of the citrate glass and the annealed product confirms the amorphous nature of the zirconium citrate complex. The powder X-ray diffraction pattern of the annealed sample indicates that it is the mixture of monoclinic and tetragonal polymorphs of zirconia. The broad nature of the peaks indicates the nanocrystalline nature of the sample. Rietveld refinement technique was used to determine the phase composition and to analyze the XRD patterns. The refinement revealed tetragonal zirconia as the major phase (92%), with approximately 8% monoclinic phase (Fig. 3). The sample shows an average crystallite size of approximately 8 nm. This small crystallite size could be the important factor in the stabilization of zirconia in the tetragonal phase. Refinement of the occupancy

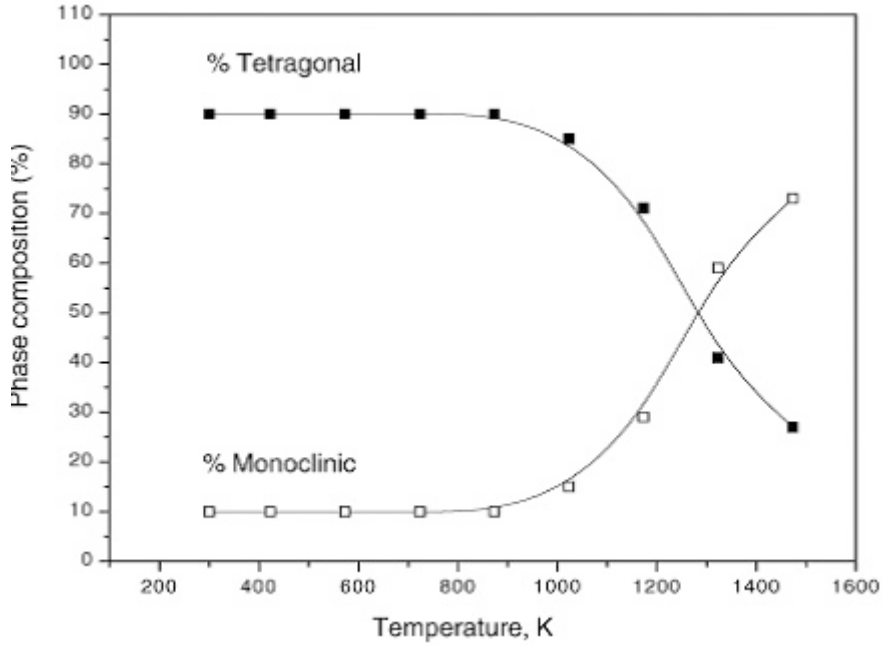

Fig. 3. Variation of the relative phase composition of the polymorph mixture as a function of temperature.

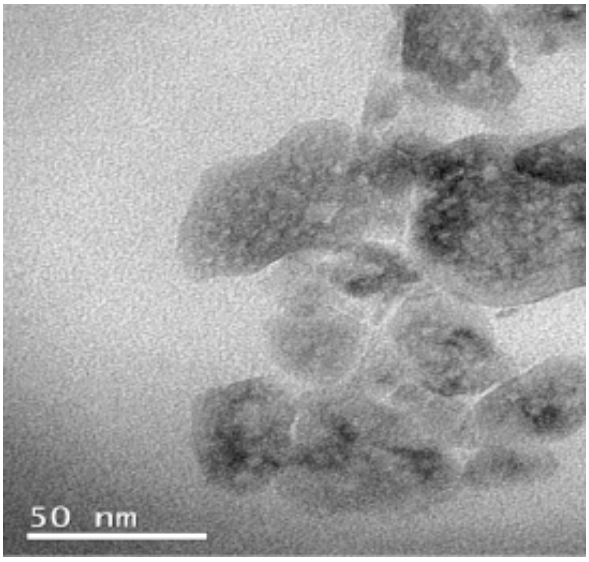

Fig. 4. Micrograph by TEM (80,000x magnification) of zirconia nanoparticles annealed at 800 °C.

factor for zirconium and oxygen atoms showed that the lattice has both cationic as well as anionic vacancies. These lattice defects could also play an important role in the stabilization to the tetragonal system along with the small crystallite size, according to Wan *et al.* [11]. Also, they have observed stabilization of zirconia, prepared by two different synthesis routes, to tetragonal phase due to the presence of large-scale lattice defects even without addition of any dopants. The *in situ* HTXRD study reveals high thermal stability of the mixture till approximately 1023K, after which the transformation of tetragonal phase into the monoclinic phase can be seen as a function of temperature till 1200 °C. This transformation is accompanied by an increase in the crystallite size of the sample. A linear increase in the lattice parameters and percent thermal expansion as a function of temperature indicates a linear lattice thermal expansion [39].

Primary particle size and agglomeration

Fig. 4 shows a micrograph obtained by transmission electronic microscopy for zirconia primary particles after annealing at 800 °C. The size of primary zirconia particle estimated through this micrograph is approximately 30 nm. This estimation is in agreement with measurement for crystallite sizes obtained by X-ray diffraction line broadening through single-line plot, assuming Pearson VII profile for size contribution. The X-ray diffraction patterns, mainly at low temperatures, showed broad peaks, indicating crystallites with average size measuring from 20 to 25 nm for monoclinic phase and from 17 to 28 nm for tetragonal phase after annealing at temperatures of 700 and 800 °C, respectively.

Sukla *et al.* [41] obtained ZrO_2 powder by sol–gel process, involving hydrolysis and condensation of zirconium (IV) *n*-propoxide in an alcohol solution, where the rate of nucleation of particles depends primarily on *R* (*R* = ratio of molar concentrations of water and zirconium IV). The ZrO_2 particles of size 200–300 nm and 15–20 nm, having tetragonal crystal structure were obtained under the processing conditions *R* = 5, [HPC] = 0.0 gL^{-1} and *R* = 30, [HPC] = 2.0 gL^{-1}, respectively. High *R*-value and high HPC concentration were observed to be conducive for the synthesis of nanocrystalline tetragonal ZrO_2 particles, resulting in higher nucleation rate of ZrO_2 nanocrystallites. In the presence of HPC polymer, these ZrO_2 nanocrystallites are sterically stabilized due to the adsorption of the HPC polymer to their surface. The aggregation of ZrO_2 primary particles is thus prevented, resulting in the formation of ZrO_2 agglomerates. The stabilization of metastable tetragonal phase in nanocrystalline ZrO_2 is the result of the minimization of surface energy. Also, from Fig. 4 it can be observed that, individual particles are being necked together. Fine particles, particularly nanoscale particles, since they have large surface areas, often agglomerate to form either lumps or secondary particles to minimize the total surface area or interfacial energy of the system [36]. Agglomeration refers to adhesion of particles to each other because of *van der Waals* forces of attraction, which is significantly higher in nanoparticles [42]. Fig. 5 shows the image obtained from scanning electronic microscopy of the zirconia powder where an appreciable formation of agglomerates after thermal treatment at 800 °C can be seen. Particle size distribution by laser diffraction indicates a mean particle size of 11.54 μm. The fundamental phenomenon involved in this case is attributed to the fact that these polycrystalline nanostructured particles grow further by coagulation and increase in surface area. The resultant larger particles eventually aggregate through a slower sintering process. It is difficult to break down an aggregated mass of nanostructured particles into the individual primary particles, and it essentially defeats the purpose of producing a high-surface-area powder [43,44].

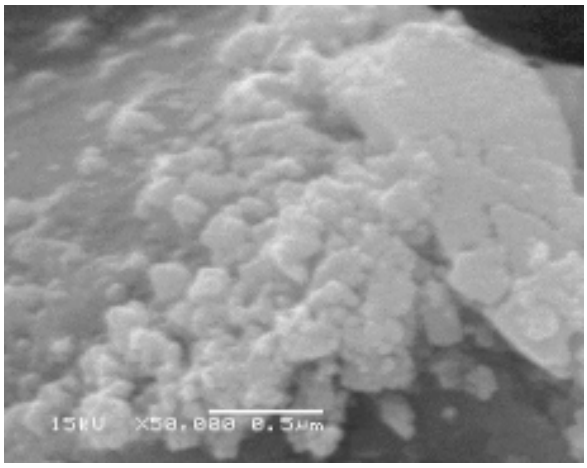

Fig. 5. Micrograph by SEM (50,000x magnification) of the sample annealed at 800 °C.

FTIR analysis of the zirconia powder

Fig. 6 shows spectra obtained by means of FTIR analysis of the zirconia powder at different temperatures ranging from 100 to 800 °C. The bands at 3380 cm^{-1} and 1565 cm^{-1} correspond to the vibration of stretching and deformation of the O-H bond due to the absorption of water and coordination water, respectively. As the annealing temperature increased, the formation of these bands gradually decreased, eventually disappearing. Another important absorption band can be observed at 466 cm^{-1}, which is related to the vibration of the Zr-O bond in ZrO_2 [45].

Zirconia membranes were prepared using zirconium butoxide via the sol–gel route. Acetic acid also served as a chelating ligand and can lead to changes in the alkoxide precursor at the molecular level, thus modifying the hydrolysis process. The FTIR analysis of zirconia xerogel shows the adsorption peaks at 1453 and 1561 cm^{-1} and clearly indicates the bidental ligand CH_3COO^-. A rapid increase in temperature (~10 °C in 10 s) also occurred when acetic acid was added to Zr butoxide/butanol mixture during our experiment. Such a phenomenon is due to the replacement of O-*n*$C_4H_9^-$ with CH_3COO^-. The hydrolysis of chelated zirconium complex (Fig. 7) is deferred so that bidental ligand may still remain in the xerogel. Upon further hydrolysis, bidental ligand is broken off and gives rise to Zr–OH bond. This mechanism decreases the rate of hydrolysis, meaning very fine particles of zirconium hydroxide will be formed and suspended in solution [46].

4. CONCLUSIONS

The nanostructured zirconia powders were obtained by sol–gel process. The structure of the zirconia produced was amorphous when the samples

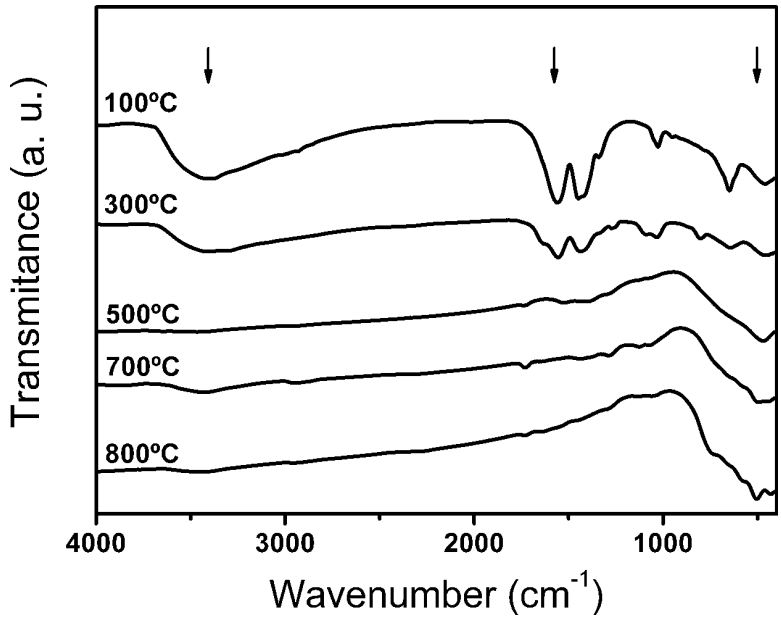

Fig. 6. FT-IR spectrum of the zirconia powder annealed at different temperatures (100, 300, 700, and 800 °C).

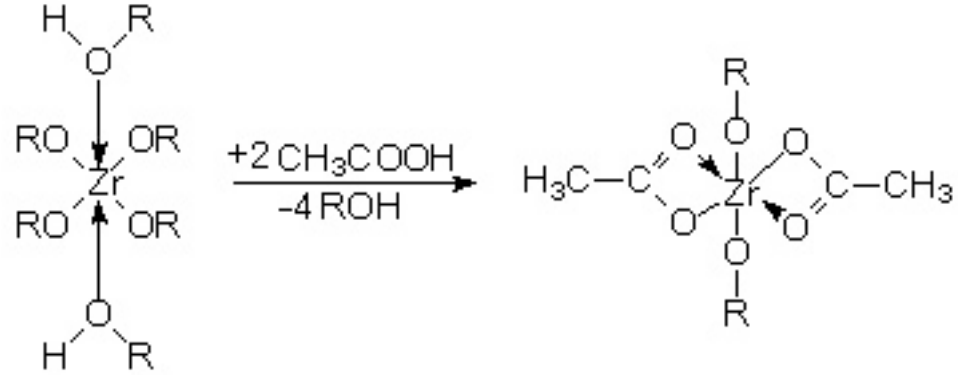

Fig. 7. Hydrolysis of chelated zirconium complex.

were heated below 400 °C. At 600 °C, the monoclinic phase was formed, resulting in the lowering of the content of tetragonal phase.

The thermogravimetric analysis showed a considerable weight loss between 40 and 200 °C, which is probably due to dehydration. An exothermic peak followed by a weight loss at approximately 450 °C is observed, which is a typical behavior related to the combustion of organic compounds. At a temperature higher than 450 °C, another exothermic peak is observed, but not followed by any weight loss, attributed to the allotropic transformation of zirconia from tetragonal to monoclinic, which is confirmed by X-ray diffraction. The water loss was confirmed in the spectrum FTIR. It was observed that the formation of the bands related to the presence of hydroxyl group showed a decrease with the increase of annealing temperatures, and at 800 °C they disappeared, showing that the material structure no longer contains zirconium hydroxide.

The crystallite size (estimated by both TEM and XDR single-line method) increases with increasing annealing temperatures: it was approximately 20–25 nm for monoclinic phase and 17–28 nm for tetragonal phase after annealing at temperatures of 700 and 800 °C, respectively. The so-obtained zirconia powders presented as micrometer-sized agglomerates (mean particle size of 11.54 μm). The

tetragonal phase was stable at 500°C because of the reduction of the surface energy, which was caused by small-sized crystallites.

REFERENCES

[1] W. Chang, G. Skandan, S. C. Danforth, M. Rose, A. G. Balogh, H. Hahn and B. Kear // *Nanostructured Mater*. **6** (1995) 321.

[2] X. C. Yang, W. Riehemann, M. Dubiel and H. Hofmeister // *Mater. Sci. Eng. B* **95** (2002) 299.

[3] S. K. Friedlander, H. D. Jang and K. H. Ryu // *Appl. Phys. Lett*. **72** (1998) 173.

[4] N. P. Rao, N. Tymiak, J. Blum, A. Neuman, H. J. Lee, S. L. Girshick, P. H. Mc Murry and J. Heberlein // *J. Aerosol Sci.* **29** (1998) 707.

[5] J. Karthikeyan, C. C. Berndt, J. Tikkanen, S. Reddy S and H. Herman // *Mater. Sci. Eng. A* **238** (1997) 275.

[6] I. Colbeck and Y. Kamlag // *J. Aerosol Sci*. **27** (1996) 395.

[7] Z. Zhang, S. Wahlberg, M. Wang and M. Muhammed // *Nanostructured Mater*. **12** (1999) 163.

[8] J. J. Kingsley and K. C. Patil // *Mater. Lett*. **6** (1988) 427.

[9] D. J. Suh, T. J. Park, J. H. Kim and K. L. Kim // *J. Non-Cryst. Solids* **225** (1998) 168.

[10] V. V. Brazhkin // *Physics-Uspekhi* **4** (2006) 719.

[11] C. J. Brinker and G. W. Scherer, *Sol-gel science, the physics and chemistry of sol-gel processing* (Academic Press, San Diego, 1990).

[12] M. Kakihana *// J. Sol-Gel Sci. Technol*. **6** (1996) 7.

[13] I. H. Kim and K. Kim // *Solid-State Le*t. **4** (2001) A62.

[14] C. Airoldi and R. F. de Farias // *Quím Nova* **27** (2004) 84.

[15] M. Curran, T. E. Gedris and A. E. Stiegman // *Chem. Mater.* **10** (1998)1604.

[16] K. Yanagisawa, Y. Yamamoto, Q. Feng and N. Yamasaki // *J. Mater. Res*. **13** (1998) 825.

[17] Z. Zhan and H. C. Zeng *// J. Non-Cryst. Solids* **243** (1999) 26.

[18] Q. Z. Yan, X. T. Su, Z. Y. Huang and C. C. Ge // *J. Eur. Ceram. Soc*. **26** (2006) 915.

[19] E. Lotero, D. Vu, C. Nguyen, J. Wagner and G. Larsen // *Chem. Mater.* **10** (1998) 3756.

[20] J. Livage and C. Sanchez // *J. Non-Cryst. Solids* **145** (1992) 11.

[21] M. Pan, J. R. Liu, M. K. Lu, D. Xu , D. R. Yuan, D. R. Chen, P. Yang and Z. H. Yang // *Thermochim Acta* **376** (2001) 77.

[22] S. Kongwudthiti, P. Praserthdam, P. Silveston and M. Inoue // *Ceram. Int*. **29** (2003) 807.

[23] X. Jiao, D. Chen and L. Xiao // *J. Cryst. Growth* **258** (2003) 158.

[24] R. Di Maggio, L. Fambri and A. Guerriero // *Chem. Mat*. **10** (1998) 1777.

[25] G. Garnweitner and M. Niederberger // *J. Am. Ceram. Soc*. **89** (2006) 1801.

[26] X. Bokhimi, A. Morales, O. Novaro, M. Portilla, T. López, F. Tzompantzi and R. Gómez // *J. Solid State Chem*. **135** (1998) 28.

[27] M. Yoshimura, S-T. Oh, M. Sando and K. Niihara // *J. Alloys Comp*. **290** (1999) 284.

[28] G. Hare'l, B.G. Ravi and R. Chaim // *Mater. Lett*. **39** (1999) 63.

[29] X. Changrog, C. Huaqiang, W. Hong, Y. Pinghua, M. Guangyao and P. Dingkun // *J. Membr. Sci.* **162** (1999) 181.

[30] J. Luo and R. Stevens // *J. Am. Ceram. Soc***. 82** (1999) 1922.

[31] W. Liu, Y. Chen, C. Ye and P. Zhang // *Ceram. Internat.* **28** (2002) 349.

[32] D. Vollath, F. D. Fischer, M. Hagelstein and D. V. Szabó // *J. Nanoparticle Res.* **8** (2006) 1003.

[33] O. Valsylkiv, Y. Sakka and V. V. Skorokhod // *J. Am. Ceram. Soc.* **86** (2003) 299.

[34] C. Viazzi, J. P. Bonino and F. Ansart // *Surf. Coat. Technol*. **201** (2006) 3889.

[35] H. Fang, T. Wan, W. Shi and M. Zhang // *J. Non-Cryst. Solids* **353** (2007) 1657.

[36] T. Ekström, C. Chatfield, W. Wruss and M. Maly-Schreiber // *J. Mater. Sci.* **20** (1985) 1266.

[37] R. Caruso, O. Sanctis, A. Macías-García, E. Benavides and R. Mintzer // J*. Mat. Proc. Technol.* **152** (2004) 299.

[38] B. Ksapabutr, E. Gulari and S. Wongkasemjit // *Powder Technol.* **148** (2004) 11.

[39] M. Bhagwat and V. Ramaswamy // *Mat. Res. Bul.* **39** (2004) 1627.

[40] C. Wan, Y. Motohashi and S. Harjo // *Mat. Trans*. **44** (2003) 1053.

[41] S. Sukla and S. Seal // *Rev. Adv. Mater. Sci.* **5** (2003) 117.

[42] A. S. Edelstein and R. C. Cammarata, *Nanomaterials: Synthesis, properties and*

applications (Bristol. IOP Publishing Ltd, 1996).
[43] M. Fan, *Ceramic and glasses, engineered materials handbook* (v. 4. New York. ASM Inter, Mater Info Soc, 1991).
[44] A. Singhal, G. Skandan, N. Wang, N. Glumac, B. H. Kear and R. D. Hunt // *Nanostructured Mater.* **4** (1999) 545.
[45] Y. Hao, J. Li, X. Yang, X. Wang and L. Lu // *Mater. Sci. Eng. A* **367**(2004) 243.
[46] J.C.-S. Wu and L.-C. Cheng // *J. Memb. Sci.* **167** (2000) 253.